

Lattice Boltzmann approach for the fluid-structure interaction of a neo-Hookean mediumErwan Liberge^{*} and Claudine Béghein[†]*LaSIE, UMR CNRS 7356, La Rochelle Université, La Rochelle, France*

(Received 4 February 2022; accepted 20 April 2022; published 23 May 2022)

In this paper, a lattice Boltzmann method (LBM) for the fluid-structure interaction of an incompressible neo-Hookean medium is proposed. The objective is to use the lattice Boltzmann method to model the fluid and the solid domains at the same time, and thus avoid coupling two solvers, one for the fluid and one for the structure. The specific case of a neo-Hookean incompressible medium allows us to use a Eulerian formulation for the structure problem, which resembles the Navier-Stokes equation. Then, a macroscopic multiphase equation can be used to model the fluid and structure problems together. Next, the LBM approach is deduced from this macroscopic multiphase formulation of the fluid-structure interaction problem. It consists in extending the LBM to the solid domain by adding a tensor term in the equilibrium function of the collision operator. The effect of the added tensor term is to cancel in the solid domain the viscous fluid constraints and add neo-Hookean constraints. Thus, only the third moment of the LBM is modified, the first two being conserved, and only the constraints in the macroscopic Navier-Stokes equation are changed. The LBM scheme obtained can then model the interaction of a fluid and a structure composed of an incompressible neo-Hookean medium with a single solver for the fluid and the solid. Two additional equations are used, one to track the fluid and solid domains with the Cahn-Hilliard equation, and the other to compute the solid displacement field by a finite-difference scheme. The proposed method is applied successfully on three cases from the literature.

DOI: [10.1103/PhysRevE.105.055307](https://doi.org/10.1103/PhysRevE.105.055307)**I. INTRODUCTION**

The classical way to simulate fluid-structure interaction (FSI) problems is to consider two solvers, one for the fluid, one for the structure, and then couple them using a synchronous or asynchronous algorithm. This approach is intuitive because of the nature of the two subproblems, the fluid being intrinsically Eulerian and the solid Lagrangian, but an efficient and fast coupling of the two solvers remains a major issue [1,2]. For a structure composed of a neo-Hookean incompressible elastic medium, although the classical equations are in a Lagrangian framework, they can be written in a Eulerian framework [3]. Thus, a multiphase formulation, which consists in extending the Navier-Stokes equations to the solid domain, can be chosen. This avoids the inherent problem of coupling two solvers and the explicit computation of the fluid forces. This approach has been used with the finite-element method and mesh refinement techniques [3] or with the immersed boundary method to enforce fluid constraints [4]. In this paper we propose to use the lattice Boltzmann method to solve this problem.

The lattice Boltzmann method (LBM) has been used in fluid mechanics since the 1990s [5] and has gained new interest with the development of computing on graphic cards (GPU). Indeed, the LBM algorithm is particularly well adapted to the GPU architecture and allows a significant gain in computing time. For these reasons, most of the classical methods used in the fluid-structure interaction (finite elements, finite volumes) have been adapted to LBM. Each time,

the displacement of the structure is solved with an external solver and the effect of the structure is modeled by bounce-back methods [6–8], immersed boundaries [9,10], or volume penalization [11,12].

We propose in this paper to treat the fluid and the solid at the same time by the lattice Boltzmann method, without using an external solver. For this purpose, a similar approach to the one proposed by Ref. [3] is used to write the macroscopic formulation of the problem. In the solid domain, the viscous stress tensor is replaced by the Eulerian neo-Hookean stress formulation. Its transcription in LBM consists in adding a tensor term which aims to remove the Cauchy constraints and add the desired term. Then, the different fluid and solid domains are followed via an interfacial evolution equation, solved here by the LBM formulation of the Cahn-Hilliard equation. A third equation is also needed to calculate the displacement field in the solid domain. This one is solved by a finite-difference scheme.

The first section presents the mathematical background, i.e., the multiphase formulation for the neo-Hookean medium in a macroscopic way. Then, the LBM model is presented, for the multiphase approach and for the Cahn-Hilliard equation. The proposed method is successfully applied to three examples from the literature.

II. THEORETICAL BACKGROUND**A. Multiphase formulation for neo-Hookean materials**

The case of a domain containing a fluid and an incompressible neo-Hookean medium is considered. The objective is to propose a monolithic formulation of the system. If we consider the equation governing the fluid domain, we obtain

^{*}erwan.liberge@univ-lr.fr[†]claudine.beghein@univ-lr.fr

the classical incompressible Navier-Stokes equations

$$\begin{aligned} \rho_f \frac{\partial \mathbf{u}_f}{\partial t} + \rho_f (\mathbf{u}_f \cdot \nabla \mathbf{u}_f) - \nabla \cdot \sigma_f &= \mathbf{f}_f \text{ in } \Omega_f, \\ \nabla \cdot \mathbf{u}_f &= 0, \end{aligned} \quad (1)$$

with associated boundary conditions, where ρ_f is the fluid density, p_f is the fluid pressure term, and σ_f the stress tensor in the fluid, defined by

$$\sigma_f = -p_f \text{Id} + 2\nu_f \mathbf{D}(\mathbf{u}_f). \quad (2)$$

μ_f is the dynamic viscosity of the fluid, Id represents the identity tensor, and $\mathbf{D}(\mathbf{u}_f)$ is the deformation rate tensor, itself defined by

$$\mathbf{D}(\mathbf{u}_f) = \frac{1}{2} (\nabla \mathbf{u}_f + \nabla^T \mathbf{u}_f). \quad (3)$$

The equation solved in the solid for \mathbf{u}_s is

$$\begin{aligned} \rho_s \frac{\partial \mathbf{u}_s}{\partial t} + \rho_s (\mathbf{u}_s \cdot \nabla \mathbf{u}_s) - \nabla \cdot \sigma_s &= \mathbf{f}_s \text{ in } \Omega_s, \\ \nabla \cdot \mathbf{u}_s &= 0. \end{aligned} \quad (4)$$

ρ_s is the solid density. For neo-Hookean incompressible materials, the stress tensor σ_s is defined by [3,4]

$$\sigma_s = -p_s \text{Id} + \mu_s (\mathbf{F}\mathbf{F}^T - \text{Id}), \quad (5)$$

and $\nabla \cdot \mathbf{u}_s = 0$. μ_s is the Lamé coefficient and \mathbf{F} is the deformation gradient tensor,

$$\mathbf{F} = (\text{Id} - \nabla \mathbf{d})^{-1}, \quad (6)$$

with \mathbf{d} the displacement field of the solid. Note that all operators are defined in a Eulerian frame.

In order to obtain a multiphase formulation, a characteristic function χ is introduced:

$$\chi(\mathbf{x}, t) = \begin{cases} 1 & \text{if } \mathbf{x} \in \Omega_s(t), \\ 0 & \text{if } \mathbf{x} \in \Omega_f(t). \end{cases} \quad (7)$$

Combining Eqs. (1) and (4), the multiphase formulation is

$$\begin{aligned} \rho \frac{\partial \mathbf{u}}{\partial t} + \rho (\mathbf{u} \cdot \nabla \mathbf{u}) - \nabla \cdot \sigma &= \mathbf{f} \text{ in } \Omega, \\ \nabla \cdot \mathbf{u} &= 0, \end{aligned} \quad (8)$$

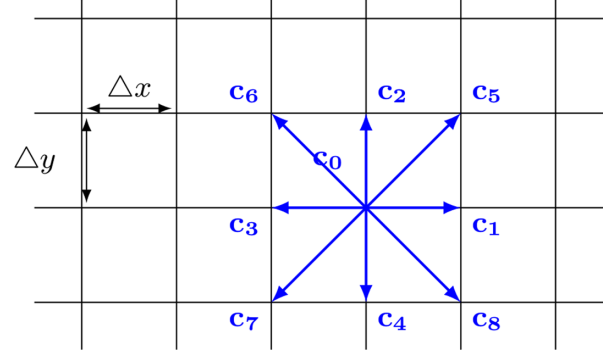


FIG. 1. Discrete velocities of the D2Q9 model.

with

$$\begin{aligned} \rho &= \rho_f(1 - \chi) + \rho_s \chi, \\ \mathbf{u} &= \mathbf{u}_f(1 - \chi) + \mathbf{u}_s \chi, \\ \sigma &= \sigma_f(1 - \chi) + \sigma_s \chi. \end{aligned} \quad (9)$$

The solid displacement is obtained using the definition of the total derivative in time:

$$\frac{\partial \mathbf{d}}{\partial t} + \mathbf{u} \cdot \nabla \mathbf{d} = \mathbf{u} \text{ in } \Omega_s. \quad (10)$$

B. LBM approach

1. LBM-TRT

Based on the Boltzmann equation [Eq. (11)], the lattice Boltzmann method has been widely used as a computational fluid dynamics (CFD) tool since the 1990s. A complete bibliography can be found in Ref. [13] to give an overview of the different variants or applications:

$$\frac{\partial f}{\partial t} + \mathbf{c} \cdot \nabla_x f = \Omega(f). \quad (11)$$

Here, we present the two relaxation time (TRT) approach that is used in this work. Let us consider the most commonly used model to simulate two-dimensional flows, the nine-velocity square lattice model D2Q9 (Fig. 1) [14].

$$\mathbf{c}_\alpha = \begin{cases} (0, 0), & \alpha = 0, \\ [\cos((\alpha - 1)\frac{\pi}{2}), \sin((\alpha - 1)\frac{\pi}{2})]c, & \alpha = 1, 2, 3, 4, \\ [\cos((2\alpha - 9)\frac{\pi}{4}), \sin((2\alpha - 9)\frac{\pi}{4})]\sqrt{2}c, & \alpha = 5, 6, 7, 8, \end{cases} \quad (12)$$

where $c = \frac{\Delta x}{\Delta t}$. Usually $\Delta x = \Delta y = \Delta t = 1$ are chosen.

We note \mathbf{c}_α the discrete velocity along the α direction and $\mathbf{c}_{\bar{\alpha}} = -\mathbf{c}_\alpha$ the discrete velocity in the opposite direction $\bar{\alpha}$.

Considering $f_\alpha(\mathbf{x}, t) = f(\mathbf{x}, \mathbf{c}_\alpha, t)$, the TRT-LBM computational scheme, for $\alpha = 0, \dots, 8$, leads to

$$f_\alpha(\mathbf{x} + \mathbf{c}_\alpha \Delta t, t + \Delta t) - f_\alpha(\mathbf{x}, t) = -\frac{\Delta t}{\tau^+} [f_\alpha^+(\mathbf{x}, t) - f_\alpha^{\text{eq}^+}(\mathbf{x}, t)] - \frac{\Delta t}{\tau^-} [f_\alpha^-(\mathbf{x}, t) - f_\alpha^{\text{eq}^-}(\mathbf{x}, t)] + \left(1 - \frac{\Delta t}{2\tau^+}\right) F_\alpha, \quad (13)$$

with

$$f_\alpha^+ = \frac{f_\alpha + f_{\bar{\alpha}}}{2}, \quad f_\alpha^- = \frac{f_\alpha - f_{\bar{\alpha}}}{2}. \quad (14)$$

In the same way, $f_\alpha^{\text{eq}+}$ and $f_\alpha^{\text{eq}-}$ are defined, with

$$f_\alpha^{\text{eq}} = \omega_\alpha \rho \left(1 + \frac{\mathbf{c}_\alpha \cdot \mathbf{u}}{c_s^2} + \frac{\mathbf{u} \mathbf{u} : (\mathbf{c}_\alpha \mathbf{c}_\alpha - c_s^2 \mathbf{I})}{2c_s^4} \right), \quad (15)$$

and the forcing term F_α is according to Guo *et al.* [15],

$$F_\alpha = \left(1 - \frac{1}{2\tau} \right) \omega_\alpha \left(\frac{\mathbf{c}_\alpha - \mathbf{u}}{c_s^2} + \frac{\mathbf{c}_\alpha \cdot \mathbf{u}}{c_s^4} \mathbf{c}_\alpha \right) \cdot \rho \mathbf{f}. \quad (16)$$

For a D2Q9 model, the weighting coefficients are

$$\omega_\alpha = \begin{cases} \frac{4}{9}, & \alpha = 0, \\ \frac{1}{9}, & \alpha = 1, 2, 3, 4, \\ \frac{1}{36}, & \alpha = 5, 6, 7, 8. \end{cases} \quad (17)$$

τ^+ is the relaxation time related to viscosity of ν :

$$\nu = c_s^2 \Delta t \left(\tau^+ - \frac{1}{2} \right). \quad (18)$$

The relaxation time τ^- is obtained as follows:

$$\tau^- = \frac{\Delta t \Lambda}{\tau^+ - \frac{1}{2}} + \frac{1}{2}. \quad (19)$$

In this work, we choose $\Lambda = \frac{1}{6}$, because of the better stability we obtained with this value.

Under the limitation of the low Mach number (\mathbf{u}/c_s), The TRT-LBM scheme leads to the incompressible Navier-Stokes equations (1). Finally, the macroscopic quantities are computed by the following expressions:

$$\rho = \sum_\alpha f_\alpha, \quad \rho \mathbf{u} = \sum_\alpha \mathbf{c}_\alpha f_\alpha + \frac{\Delta t}{2} \rho \mathbf{f}. \quad (20)$$

2. LBM for Cahn-Hilliard equation

To avoid the difficulties inherent in solving the advection of the sharp function χ , the diffuse interface method is used. We define a smooth function ϕ that follows a Cahn-Hilliard equation (CHE) [16]:

$$\frac{\partial \phi}{\partial t} + \mathbf{u} \cdot \nabla \phi = M \nabla^2 \mu_\phi. \quad (21)$$

M is the mobility parameter and μ_ϕ the chemical potential is defined as follows:

$$\mu_\phi = 4\beta(\phi - \phi_{\Omega_s})(\phi - \phi_{\Omega_f})(\phi - \bar{\phi}) - k \nabla^2 \phi. \quad (22)$$

β and k are parameters related to the interface thickness W and the surface tension force σ , ϕ_{Ω_f} (respectively ϕ_{Ω_s}) is the value defined to mark the domain Ω_f (respectively Ω_s), and $\bar{\phi} = (\phi_{\Omega_f} + \phi_{\Omega_s})/2$. In the context of multiphase fluid flows, β and k have a physical meaning:

$$W = \frac{4}{|\phi_{\Omega_s} - \phi_{\Omega_f}|} \sqrt{\frac{k}{2\beta}} \quad \text{and} \quad \sigma = \frac{|\phi_{\Omega_s} - \phi_{\Omega_f}|^3}{6} \sqrt{2k\beta}. \quad (23)$$

This allows us to define the Peclet number $\text{Pe} = U_0 W / [M\beta(\phi_{\Omega_s} - \phi_{\Omega_f})^2]$.

In the present work, interfacial forces compete with the difference in stresses in the fluid and solid domains. We assume that the interfacial forces are negligible compared to the stresses in the solid domain. The present study is closer

to the case of a fluid-rigid body interaction than a fluid-fluid interaction. This means that these parameters are chosen in such a way that they have no influence on the overall system. Another point is that the parameters k and β are chosen to decrease the artificial Peclet number of the simulation in order to improve the stability of the calculation.

The function ϕ is defined in the initial step as

$$\phi(\mathbf{x}, 0) = \begin{cases} \tanh\left(\frac{2\|\mathbf{x} - \gamma(0)\|}{W}\right) & \text{if } \mathbf{x} \in \Omega_s(0), \\ -\tanh\left(\frac{2\|\mathbf{x} - \gamma(0)\|}{W}\right) & \text{if } \mathbf{x} \in \Omega_f(0), \end{cases} \quad (24)$$

where $\gamma(0)$ is the position of the fluid-solid interface at $t = 0$. Then, the values of ϕ are always between -1 and 1 , and thus the transition between Ω_f and Ω_s is smooth.

Once ϕ is calculated, the following calculation is used to adjust the function χ between 0 and 1:

$$\chi = -\frac{\phi - \phi_{\Omega_s}}{\phi_{\Omega_f} - \phi_{\Omega_s}} + 1. \quad (25)$$

Then χ can be used directly in Eqs. (9).

The LBM approach for CHE proposed by Zu *et al.* [17] is used,

$$\begin{aligned} g_\alpha(\mathbf{x} + \mathbf{c}_\alpha \Delta t, t + \Delta t) - g_\alpha(\mathbf{x}, t) &= -\frac{g_\alpha(\mathbf{x}, t) - g_\alpha^{\text{eq}}(\mathbf{x}, t)}{\tau_g} + (2\tau_g - 1) \\ &\quad \times [g_\alpha^{\text{eq}}(\mathbf{x} + \mathbf{c}_\alpha \Delta t, t) - g_\alpha^{\text{eq}}(\mathbf{x}, t)], \end{aligned} \quad (26)$$

where $\phi = \sum_\alpha g_\alpha$, $M = (\tau_g - 1/2)\Gamma \Delta t$, and Γ is a numerical parameter controlling the mobility M and

$$g_\alpha^{\text{eq}} = \begin{cases} \phi + \frac{(1-\omega_0)\Gamma\mu_\phi}{2(\tau_g-1)c_s^2}, & \alpha = 0, \\ -\omega_\alpha \frac{\Gamma\mu_\phi + (\mathbf{c}_\alpha \cdot \mathbf{u})\phi}{2(\tau_g-1)c_s^2} & \alpha \neq 0. \end{cases} \quad (27)$$

3. Multiphase LBM formulation FSI with neo-Hookean formulation

Consider a LBM formulation for Eq. (4) with the constraint tensor (5). The approach is to remove the viscous constraint tensor τ_s^v and add σ_s .

Let $\tau_s^v = 2\nu_f \mathbf{D}(\mathbf{u}_s)$ and $\tau_s^\mu = \mu_s(\mathbf{F}\mathbf{F}^T - \text{Id})$. τ_s^v can be computed with the distribution functions f_α , which avoids computing explicitly spatial derivatives:

$$\tau_s^v = -\left(1 - \frac{1}{2\tau} \right) \sum_\alpha \mathbf{c}_\alpha \otimes \mathbf{c}_\alpha (f_\alpha - f_\alpha^{\text{eq}}). \quad (28)$$

Let us define the tensor \mathbf{T} :

$$\mathbf{T} = \tau_s^v - \tau_s^\mu. \quad (29)$$

The equilibrium functions are modified so that only the third moment is changed:

$$\tilde{f}_\alpha^{\text{eq}} = \omega_\alpha \rho \left(1 + \frac{\mathbf{c}_\alpha \cdot \mathbf{u}}{c_s^2} + \frac{(\mathbf{u} \otimes \mathbf{u} + \frac{\mathbf{T}}{\rho}) : (\mathbf{c}_\alpha \otimes \mathbf{c}_\alpha - c_s^2 \mathbf{I})}{2c_s^4} \right). \quad (30)$$

This leads to affect the third moment:

$$\Pi_{ij}^{\text{eq}} = \sum_\alpha \tilde{f}_\alpha^{\text{eq}} c_{\alpha i} c_{\alpha j} = \rho u_i u_j + \rho c_s^2 \delta_{ij} + T_{ij}. \quad (31)$$

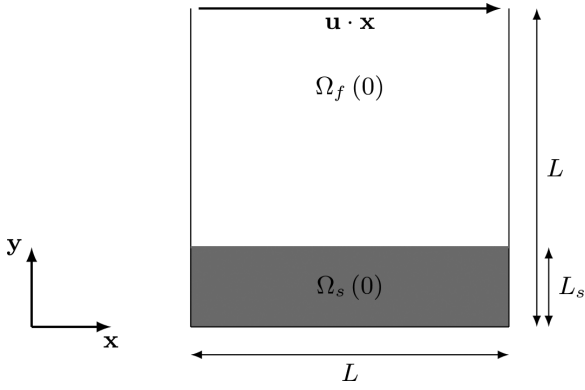


FIG. 2. Lid driven cavity with neo-Hookean structure at the bottom.

This leads to modify the macroscopic Navier-Stokes equation by adding $-\nabla \cdot \mathbf{T}$:

$$\rho_s \frac{\partial \mathbf{u}_s}{\partial t} + \rho_s (\mathbf{u}_s \cdot \nabla \mathbf{u}_s) = -\nabla p + \nabla \cdot \tau_s^v - \nabla \cdot \mathbf{T} + \mathbf{f}_s \text{ in } \Omega_s. \quad (32)$$

Considering Eq. (29), we obtain the following equation:

$$\rho_s \frac{\partial \mathbf{u}_s}{\partial t} + \rho_s (\mathbf{u}_s \cdot \nabla \mathbf{u}_s) = -\nabla p + \nabla \cdot \tau_s^\mu + \mathbf{f}_s \text{ in } \Omega_s. \quad (33)$$

The term τ_s^μ is calculated using a finite-difference scheme.

Let us note $d_\beta^{i,t+1} = d_\beta(x_i, t + \Delta t)$. Equation (10) is solved using an explicit finite-difference scheme:

$$d_\beta^{i,t+1} = d_\beta^{i,t} + \Delta t (u_\beta^{i,t} - u_1^{i,t} d_{\beta,1}^{i,t} - u_2^{i,t} d_{\beta,2}^{i,t}). \quad (34)$$

Depending on the sign of $u_1^{i,t}$ and $u_2^{i,t}$, we choose an upwind or downwind discretization scheme for $d_{\beta,1}^{i,t}$ and $d_{\beta,2}^{i,t}$.

Let us summarize the algorithm:

Algorithm 1. One time step.

$\rho(t)$, $\mathbf{u}(t)$, $\chi(t)$, and $\mathbf{d}(t)$ are known.

1. Compute \mathbf{T} [Eq. (29)].
2. Compute $\rho(t + \Delta t)$ and $\mathbf{u}(t + \Delta t)$ [Eq. (13)] with

$$f_\alpha^{\text{eq}} = (1 - \chi) f_\alpha^{\text{eq}} + \chi \tilde{f}_\alpha^{\text{eq}}. \quad (35)$$

3. Compute $\mathbf{d}(t + \Delta t)$ [Eq. (10)].
4. Compute $\phi(t + \Delta t)$ and $\chi(t + \Delta t)$ [Eq. (26)].

Note that the fluid constraints on the fluid-structure interface do not need to be computed explicitly. They are intrinsic to the proposed formulation. It is one of the interests of this approach.

III. APPLICATIONS

All computations were performed on a NVIDIA QUADRO P500 GPU card, using a CUDA implementation.

A. Lid driven cavity with neo-Hookean structure at the bottom

This first application was studied by Dunne [3], Wang *et al.* [18], Zhang *et al.* [19], and Zhao *et al.* [4]. Velocity is imposed at the top of the cavity (Fig. 2), and the resulting flow deforms

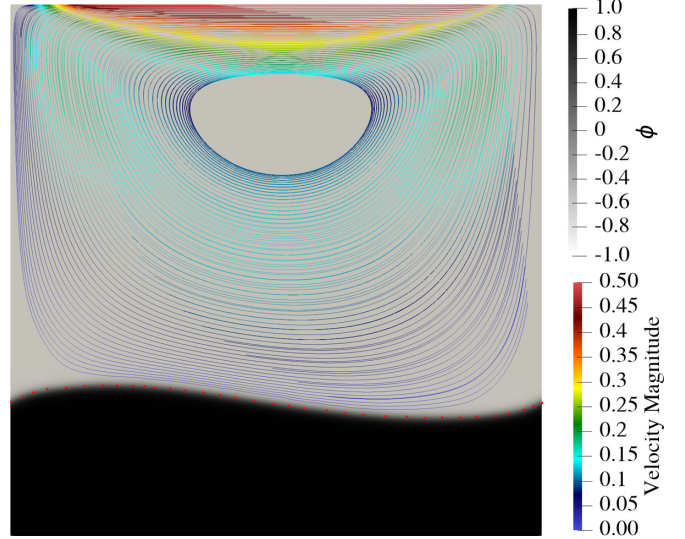


FIG. 3. Streamlines and function ϕ at a physical time $t = 8$ s (stationary solution), and \blacksquare stationary interface from Ref. [4] (application A).

the elastic bottom to a stationary configuration. The physical parameters are as follows: $L = 2$ cm; $L_s = 0.5$ cm, $\rho_f = \rho_s = 1$ g cm $^{-3}$, $\nu_f = 0.2$ dyn s cm $^{-2}$, and $\mu_s = 0.2$ dyn cm $^{-2}$, and

$$\mathbf{u}(x, L, t) = U_0 \begin{cases} \sin^2(\pi x/0.6)\mathbf{x}, & x \in [0.0, 0.3], \\ \mathbf{x}, & x \in [0.3, 1.7], \\ \sin^2(\pi(x-2)/0.6)\mathbf{x}, & x \in [1.7, 2]. \end{cases} \quad (36)$$

The LBM parameters are in lattice units (l.u.): $L_{\text{LBM}} = 200$, $\rho_{\text{LBM}} = 1$, $U_{0\text{LBM}} = 0.011$, $\nu_{f\text{LBM}} = 0.447$, $\mu_{s\text{LBM}} = 0.0001$.

The parameters of the LBM model are chosen such that the mass ratios between the fluid and solid phase and the Reynolds number are conserved. We first choose the density of the LBM model. We fix it at $\rho_{\text{LBM}} = 1$, which is classical in lattice Boltzmann methods. Then, the size of the discretized model, i.e., the number of nodes in the lattice, is fixed by the value of L_{LBM} . The last parameter we need to control is $\mu_{s\text{LBM}}$, because a too small value could make the constraint τ_s^μ numerically negligible compared to τ_s^v in expression (29). Next, we compute $U_{0\text{LBM}}$ using the nondimensional definition of the parameters defined earlier:

$$U_{0\text{LBM}} = \sqrt{\frac{\nu_{s\text{LBM}} \rho_s U_0^2}{\rho_{\text{LBM}} \mu_s}}. \quad (37)$$

Finally, the viscosity of the LBM model (and thus the relaxation time) is obtained from the conservation of the Reynolds number.

The solution obtained at physical time $t = 8$ s is rescaled to the physical parameters and plotted in Fig. 3. The position of the interface is compared with that obtained by Zhao *et al.* [4] (\blacksquare red square) at the same physical time. A good agreement is found between our result and the literature. The solution obtained here is also stationary since approximatively the time $t = 6$ s (Fig. 4). We can see that due to the fluid flow, the solid domain sinks in on the right-hand side and rises on the left-hand side. The streamlines show that there is no

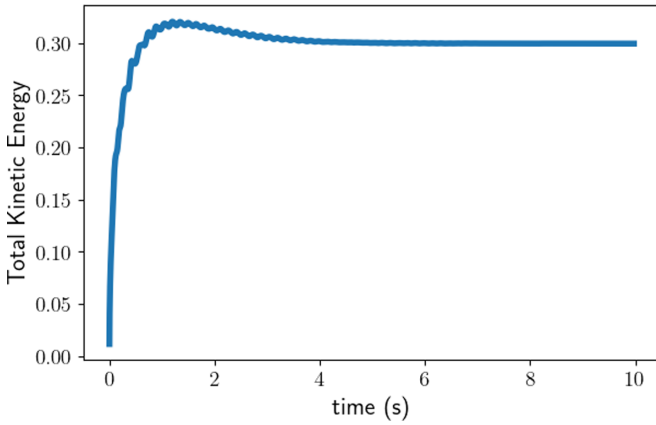


FIG. 4. Energy vs time (application A). The solution becomes stationary around 6 s.

penetration of the fluid into the solid and that physically the two domains are well separated.

B. Cavity with normal fluid flow

The second application focuses on the $L \times L$ square cavity (Fig. 5) with a periodic normal velocity imposed at the inlet:

$$\mathbf{u}(x, L) = -U_0[1 - \cos(2\pi t)] \sin(2\pi x)\mathbf{y}. \quad (38)$$

Periodic conditions are imposed on the left and right boundaries, and at the initial time, the velocity field in the cavity is equal to 0. The physical parameters are as follows: $L = 1$ m, $L_s = 0.5L$, $U_0 = 1$ m s⁻¹, $\rho_f = \rho_s = 1$ kg m⁻³, $\nu_f = 0.001$ Pa s, $\mu_s = 0.25$ Pa.

The LBM parameters used here are as follows: $L = 400$, $U_0 = 0.1265$, $\nu_{fLBM} = 0.2529$, $\mu_{sLBM} = 0.001$. In the previous application, the fluid flows tangentially along the boundary, and the deformation of the solid is due to the shear, with relatively low velocities. In the current case, the fluid hits the solid on the left-hand side of the cavity, and sucks on the right-hand side. In addition, the fluid that flows at the inlet is nonstationary, which increases the stress on the

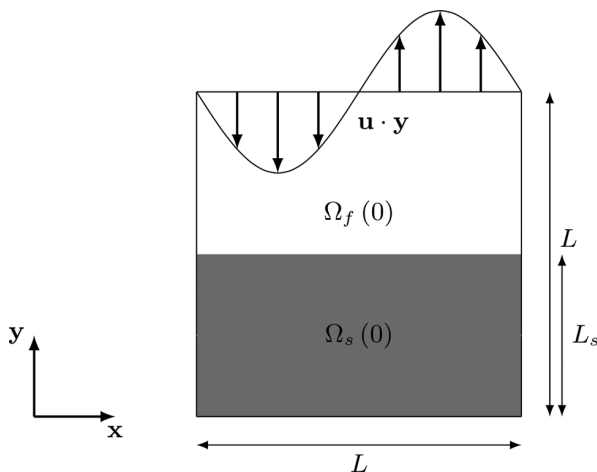


FIG. 5. Square cavity with time-periodic inlet velocity and neo-Hookean structure at the bottom.

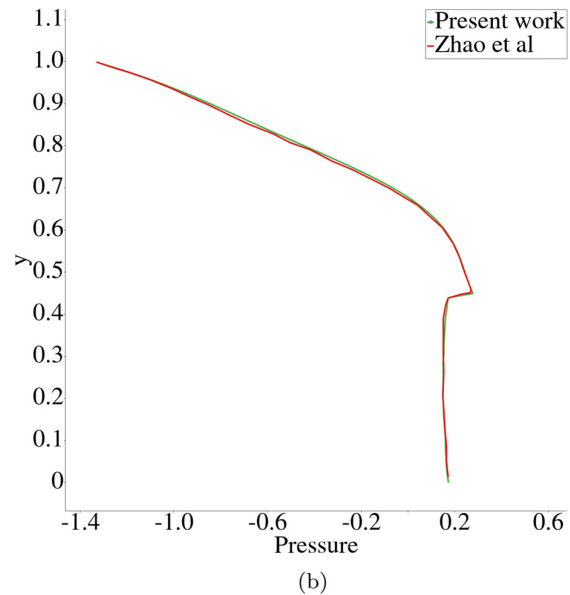
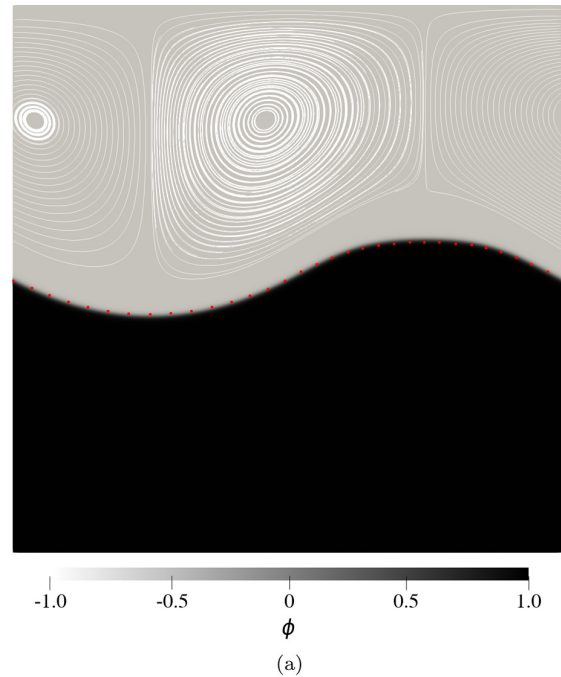


FIG. 6. Solution of application B compared to Zhao *et al.* [4]. Deformation of the elastic wall at physical time $t = 1$ s, (■): solution obtained in [4] and (b) Pressure on $x = 0.25$ at physical time $t = 0.75$ s.

structure. Under the effect of fluid stresses, the neo-Hookean medium sinks on the left, and under the effect of suction and incompressibility of the medium, the right-hand side rises. The results obtained are compared with those of Zhao *et al.* [4] (Fig. 6). At a physical time $t = 1$ s, the same interface position is obtained [Fig. 6(a)], which means that the same behavior of the fluid-structure problem is modeled. We can also observe that the streamlines and the vortex positions are identical. In Fig. 6(b), the pressure distribution on a line at $x = 0.25$ and time $t = 0.75$ s is also compared. Note that in order to analyze

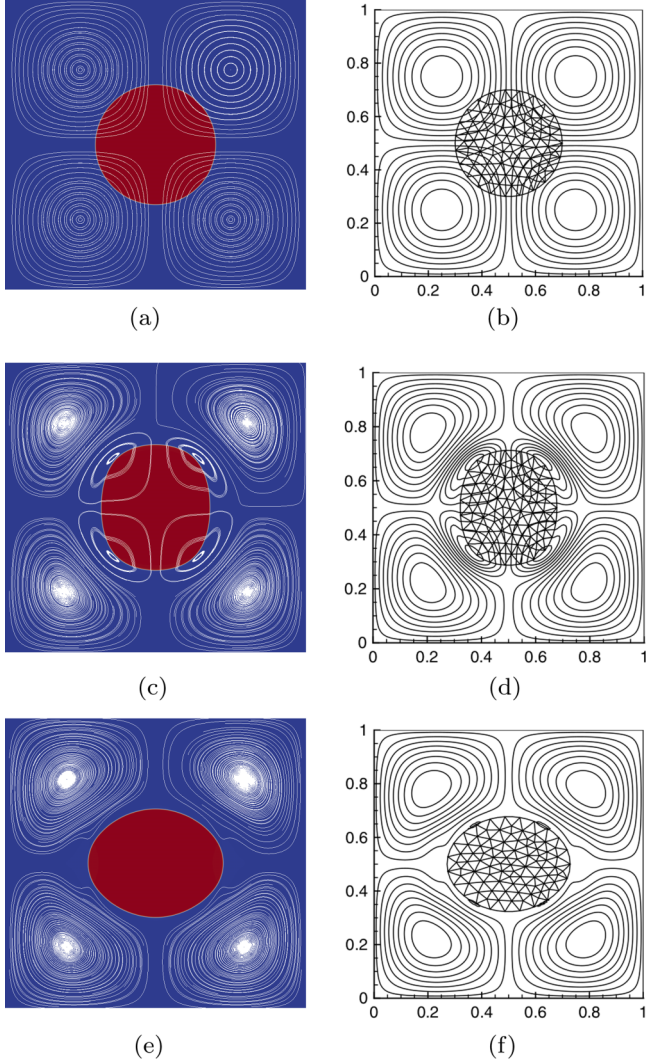


FIG. 7. Application C: Comparison of results obtained with Zhao *et al.* [4]. (a) Present work: $t = 0$ s, (b) Zhao *et al.*: $t = 0$ s, (c) Present work: $t = 0.5$ s, (d) Zhao *et al.*: $t = 0.5$ s, (e) Present work: $t = 1$ s, and (f) Zhao *et al.*: $t = 1$ s.

the pressure distribution, the value obtained by the LBM is rescaled to be compared with the literature data. We observe that a similar result from the literature is also obtained. The pressure jump at the interface is well captured, and fits well with the reference.

C. Oscillating disk

The last example concerns an oscillating disk in a periodic square cavity. Initially, the disk is located at the center of the cavity and is stress free. An initial velocity field is applied both to the fluid and the solid according to the stream function,

$$\phi(x, y) = \phi_0 \sin(2\pi x) \sin(2\pi y), \quad (39)$$

where $\phi_0 = 5 \times 10^{-2}$. The physical properties are $\rho_s = \rho_f = 1 \text{ kg m}^{-3}$, $\nu_f = 0.001 \text{ Pa s}$, $\mu_s = 1 \text{ Pa}$, and the disk radius is $r = 0.2 \text{ m}$.

Due to the initial velocity field, the disk starts to stretch along the x axis from 0 to 0.2 s. Then, the neo-Hookean

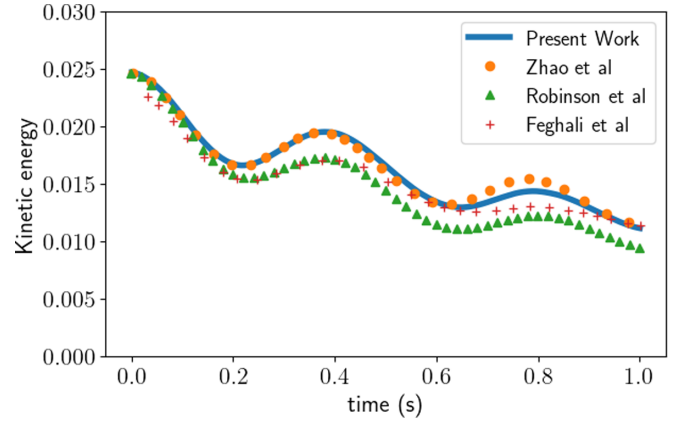


FIG. 8. Application C: Comparison of the kinetic energy obtained with the literature [4,20,21].

stresses are dominant, the solid contracts, and begins the oscillatory behavior. The results at three different times are compared with those of Ref. [4] in Fig. 7 with good agreements. The same streamlines and solid deformations are obtained. As Zhao *et al.* [4], the discontinuity of the velocity gradient can be seen by the change of the streamlines at the fluid-solid interface.

The kinetic energy is also compared in Fig. 8, with good agreement with the results in the literature [4,20,21]. The kinetic energy decreases with oscillation. Local maxima and minima correspond to stretching along the x and y axes. Robinson *et al.* [21] used a monolithic approach for the FSI problem, and they noted that the treatment of the advection term in the fluid solver would be the cause of the additional damping observed. Feghali *et al.* [20] used a linearized model for the small displacements of the structure using a finite-element approach, which could explain the differences observed in this study. Finally, our results are very close to those of Zhao *et al.* [4], even though an overdamping is observed after a time 0.6 s. However, this variation is of the order of what can be observed in Zhao's study when the mesh size and the number of Lagrangian markers used for the structure are changed.

IV. CONCLUSION

We have proposed a multiphase LBM method to model the interaction between a fluid and a structure consisting of an incompressible neo-Hookean medium. This LBM approach is based on existing work on the neo-Hookean medium at the macroscopic scale. First, a Eulerian formulation of the structure problem is used. A Navier-Stokes-like equation is obtained for a neo-Hookean medium. The difference with the classical Navier-Stokes equation lies in the stress tensor, which is not the Cauchy stress tensor but the Eulerian writing of the neo-Hookean stress tensor. Combined with the Navier-Stokes equation for the fluid, a multiphase formulation for the fluid-structure interaction is obtained [3].

A LBM formulation is built by adding in the equilibrium function a tensor, such that only the third moment is modified. The interest is that the fluid forces acting on the structure do not need to be computed explicitly. They are intrinsic to

the formulation. The model needs two other equations, one to track the domains, which is solved using a Cahn-Hilliard approach, and the last one to compute the Eulerian displacement field, which is solved with an explicit finite-difference scheme.

The method proposed is applied, on a GPU device, to three cases from the literature. The first one is a driven cavity, whose bottom is in a neo-Hookean material. The computation

converges to a stationary solution. The second example is a periodic square cavity with a normal nonstationary inlet velocity, and a neo-Hookean medium bottom. The solution obtained is also in good agreement with the literature. The last example is an oscillating disk in a periodic fluid flow. Initially, the disk is stress free, and due to the fluid flow, the disk stretches alternately along the x and y axes. The same streamlines of the literature are obtained.

-
- [1] E. H. van Brummelen and C. Farhat, *Int. J. Numer. Methods Eng.* **122**, 5173 (2021).
 - [2] A. Naseri, O. Lehmkuhl, I. Gonzalez, E. Bartrons, C. D. Pérez-Segarra, and A. Oliva, *J. Fluids Struct.* **80**, 94 (2018).
 - [3] T. Dunne, *Int. J. Numer. Methods Fluids* **51**, 1017 (2006).
 - [4] H. Zhao, J. Freund, and R. Moser, *J. Comput. Phys.* **227**, 3114 (2008).
 - [5] R. Benzi, S. Succi, and M. Vergassola, *Phys. Rep.* **222**, 145 (1992).
 - [6] A. Ladd and R. Verberg, *J. Stat. Phys.* **104**, 1191 (2001).
 - [7] M. Bouzidi, M. Firdaouss, and P. Lallemand, *Phys. Fluids* **13**, 3452 (2001).
 - [8] D. Noble and J. Torczynski, *Int. J. Mod. Phys. C* **9**, 1189 (1998).
 - [9] Z.-G. Feng and E. Michaelides, *J. Comput. Phys.* **195**, 602 (2004).
 - [10] Y. Wang, C. Shu, C. Teo, and J. Wu, *J. Fluids Struct.* **54**, 440 (2015).
 - [11] M. Benamour, E. Liberge, and C. Béghein, *J. Comput. Sci.* **39**, 101050 (2020).
 - [12] M. Benamour, E. Liberge, and C. Béghein, *Int. J. Multiphys.* **9**, 299 (2015).
 - [13] T. Kruger, H. Kusumaatmaja, A. Kuzmin, O. Shardt, G. Silva, and E. M. Viggen, *The Lattice Boltzmann Method - Principles and Practice*, Graduate Texts in Physics (Springer, Berlin, 2017).
 - [14] D. Yu, R. Mei, L.-S. Luo, and W. Shyy, *Prog. Aerosp. Sci.* **39**, 329 (2003).
 - [15] Z. Guo, C. Zheng, and B. Shi, *Phys. Rev. E* **65**, 046308 (2002).
 - [16] L. Cherfils and M. Petcu, *Commun. Pure Appl. Anal.* **15**, 1419 (2016).
 - [17] Y. Q. Zu and S. He, *Phys. Rev. E* **87**, 043301 (2013).
 - [18] X. Wang and L. T. Zhang, *Comput. Mech.* **45**, 321 (2009).
 - [19] Z.-Q. Zhang, G. R. Liu, and B. C. Khoo, *Int. J. Numer. Methods Eng.* **90**, 1292 (2012).
 - [20] E. Hachem, S. El Feghali, T. Coupez, and R. Codina, *Int. J. Numer. Methods Eng.* **104**, 566 (2015).
 - [21] A. Robinson-Mosher, C. Schroeder, and R. Fedkiw, *J. Comput. Phys.* **230**, 1547 (2011).